A mechanism for localised lignin deposition in the endodermis

Yuree Lee[1], Maria C. Rubio[1,2], Julien Alassimone[1], Niko Geldner[1*]

[1]Department of Plant Molecular Biology, University of Lausanne, UNIL–Sorge, Biophore Building, 1015 Lausanne, Switzerland

[2]Departamento de Nutrición Vegetal, Estación Experimental de Aula Dei, Consejo Superior de Investigaciones Científicas, Apdo 13034, 50080 Zaragoza, Spain

[*]autor for correspondence : Niko.Geldner@unil.ch

Abstract

The precise localisation of extracellular matrix and cell wall components is of critical importance for multicellular organisms. Lignin is a major cell wall modification that often forms intricate subcellular patterns that are central to cellular function. Yet, the mechanisms of lignin polymerisation and the subcellular precision of its formation remain enigmatic. Here we show that the Casparian strip, a lignin-based, paracellular diffusion barrier in plants, forms as a precise, median ring by the concerted action of a specific, localised NADPH oxidase, brought into proximity of localised peroxidases through the action of CASPARIAN STRIP DOMAIN PROTEINS (CASPs). Our findings in Arabidopsis provide a simple mechanistic model of how plant cells regulate lignin formation with subcellular precision. We speculate that scaffolding of NADPH oxidases to the downstream targets of the reactive oxygen species (ROS) they produce might be a widespread mechanism to ensure specificity and subcellular precision of ROS action within the extracellular matrix.

Introduction

Localised deposition and modification of extracellular matrix is crucial for the correct development and function of multi-cellular organisms. In animals, the many-faceted roles of the extracellular matrix include providing cues for cellular migration, cell layer communication or even controling the spread and activity of morphogenic signals (Kim et al., 2011). Consequently, deregulation of matrix function can be intimately associated with tumor development. In plants, the highly turgescent cells undergo localised loosening, strengthening or modification of the cell wall to drive morphogenesis of individual cells, as well as controling the integrity of entire cell layers and organs (Cosgrove, 2005). Dramatic examples of highly localised loosening of cell walls are found in tip growing root hair cells and pollen tubes (Foreman et al., 2003; Monshausen et al., 2007; Swanson and Gilroy, 2010). Just as dramatic is the contact signal-dependent rupture of the pollen cell wall upon encounter of the female embryo sac and the explosive release of the sperm cells (Boisson-Dernier et al., 2009; Escobar-Restrepo et al., 2007; Miyazaki et al., 2009). The stomatal pores that regulate gas exchange across the leaf epidermis display a precisely localised separation of certain cell wall regions and thickening of others, both of which are crucial for the functionality of these pores (Bergmann and Sack, 2007). Xylem vessels result from an apoptotic program that leaves behind a strongly thickened but intricately structured set of interconnected hollow tubes that mediate nutrient and water flow within the plant (Oda and Fukuda, 2012b). Plant cells detect and respond to cell wall manipulations by pathogens with rapid deposition of altered and strenghtened cell walls at sites of infection (Hematy et al., 2009). In all these examples, we are only beginning to identify the underlying molecular factors and we are largely ignorant about how localised modifications of cell walls can be achieved.

Lignin deposition is a major cell wall modification that plants employ in many different cell types and in response to various environmental stresses. Added to the fundamental importance of lignin is a biotechnological incentive to manipulate lignin formation, as it remains a major obstacle for the utilisation of cellulosic biofuels (Vanholme et al., 2010). Lignin formation has been studied extensively as part of xylem differentiation. However, the intricate subcellular patterns observed in this system are rather a result of the prior formation of localised secondary cellulosic walls (Oda and Fukuda, 2012a, b). The formation of lignin *per se* was recently shown to be post-apoptotic in differentiating xylem vessels. It is unclear to which degree polymerisation of lignin itself is spatially controlled in these cells (Pesquet et al., 2010) and which factors would locally initiate or restrict lignin polymerisation. Understanding localised lignin formation is also hindered by the many uncertainties concerning the general mechanisms of lignin polymerisation in vivo (Liu, 2012). While it is well established that peroxidases and laccases catalyse oxidative coupling of mono-lignols *in vitro*, evidence for their role *in planta* has been more difficult to obtain. Recently, a laccase double mutant in Arabidopsis was shown to have significantly lower lignin content, providing *in vivo* evidence for laccases in lignin formation (Berthet et al., 2011). In the case of peroxidases, a high degree of genetic

redundancy seems to have precluded identification of similarly strong lignin phenotypes and current evidence is restricted to a number of RNA interference approaches which reported variable effects on lignin content (Fagerstedt et al., 2010; Liu, 2012). The source of hydrogen peroxide that would be required for peroxidase activity has also remained an open question. Plasma membrane localised NADPH oxidases have been implicated in production of reactive oxygen species (ROS) during lignification, but this has been entirely based on inhibitor studies and no specific NADPH oxidase (called Respiratory burst oxidase homologs, RBOHs, in plants) has been shown to provide ROS for lignin formation (Barcelo, 1998; Karkonen and Koutaniemi, 2010)

Recently, it has been demonstrated in Arabidopsis that Casparian strips in endodermal cells are lignin-based structures (Naseer et al., 2012). Casparian strips represent highly localised modifications of the primary cell walls that surround individual cells in a median position and confer paracellular (apoplastic) barrier properties to endodermal cells. The endodermis is a fundamental cell layer in the roots of vascular plants, which resembles polarised epithelia of animals, both in structure and function (Alassimone et al., 2010; Roppolo et al., 2011). A family of previously unknown, small transmembrane proteins has been identified, which predict the localised formation of Casparian strips and are necessary for its correct formation (Roppolo et al., 2011). These **CA**sparian **S**trip Domain **P**roteins, CASPs, were proposed to form an extensive, transmembrane polymeric platform and were speculated to guide the assembly and activity of lignin biosynthetic enzymes.

Here we demonstrate that CASP1 is a determinant for the subcellular localisation of a specific endodermal peroxidase. In addition, we reveal that mutations in one of the NADPH oxidase family members of Arabidopsis strongly delays formation of Casparian strips. This NADPH oxidase is recruited into the Casparian strip domain, and we show that a combination of specific N-terminal regulatory domain and subcellular localisation determines its non-redundant activity. Based on our data we can draw a model whereby subcellular precision of lignin polymerisation is achieved by the combinatorial action of a locally restricted production of ROS substrate and localised peroxidase activity, brought together by the scaffolding activity of CASPs.

Results

A specific NADPH oxidase is required for Casparian strip formation

In order to identify factors involved in Casparian strip formation, we undertook a forward genetic screen for mutants with an impaired endodermal barrier. We identified 11 mutants out of an EMS-population of more than 20000 lines (Alassimone et al., *unpublished*). Six of these lines formed the single, largest complementation group. We were able to rapidly determine the identity of this s*chengen4 (sgn4)* complementation group, due to its phenotypic similarity with a T-DNA insertion line in the *Respiratory burst oxidase homolog F (RBOHF)* gene, investigated as part of a parallel, reverse genetic approach in our group. The mutants were termed “Schengen” after the treaty that established a borderless area between European member states. Non-complementation with the *rbohf* T-

DNA allele and identification of either stop – or missense mutation in the *RBOHF* sequence of all six alleles demonstrated that *SGN4* is identical to *RBOHF* (Figure 1A, Table S1 and S2). *sgn4*/*rbohf* mutants show a very strong delay in the formation of an apoplastic diffusion barrier, as visualised by the penetration of externally applied propidium iodide (PI) into the stele - a convenient assay for presence of a functional endodermal diffusion barrier (Alassimone et al., 2010; Naseer et al., 2012) (Figure 1B). The defective barrier is due to a complete absence of the Casparian strip in younger root parts, visualised by its autofluorescence after clearing (Figure 1C). Eventually, aberrantly structured Casparian strips form in older parts of the root, which eventually will succeed in effectively blocking penetration of PI into the stele. A similarly strong delay in the block of PI uptake (block at 36.3±0.5 cells) can be observed in a *casp1 casp3* double mutant (Hosmani et al., *unpublished*). In this case, however an aberrant, patchy Casparian strip-like structure is formed (Roppolo et al., 2011). We tested whether SGN4/RBOHF is required for the expression, accumulation or localisation of the CASPs, which could cause the observed delay in Casparian strip formation. However, CASP1-GFP showed a normal accumulation and localisation in the mutant (Figure 1D). Consistently, protein exclusion of generic plasma membrane markers and confinement of polarly localised proteins still occurs in *rbohf* (Figure S1), suggesting that the Casparian strip membrane domain (CSD) is present and functional. This places RBOHF downstream of the formation of the localised CASP platform, suggesting a role in the execution of the cell wall formation, guided by the CASPs.

NADPH oxidase-dependent localised H_20_2 production at Casparian strips

Lignin formation requires oxidation of mono-lignols, which is thought to be catalysed by peroxidases. Peroxidases require hydrogen peroxide (H_20_2) for this oxidation and NADPH oxidases have been implicated as major sources of regulated superoxide production, which can be enzymatically or non-enzymatically dismutated into H_20_2. Therefore, we considered it most straightforward that SGN4/RBOHF would be needed for the production of H_20_2 as a peroxidase co-substrate. In this scenario RBOHF has a very direct role and even short-term inhibition of the NADPH oxidase should be able to block Casparian strip formation. The NADPH oxidase inhibitor Diphenylene iodonium (DPI) allows to precisely time the inhibition of NADPH oxidase activity, but its general effect on all NADPH oxidases severely inhibits root growth and causes cell death after prolonged treatment, making it difficult to analyse slow developmental processes (Figure S2). We therefore resorted to a recently developed short-term assay for Casparian strip formation (Naseer et al., 2012). For this, seedlings are grown for 24 hours on the mono-lignol biosynthesis inhibitor, piperonylic acid. Cells that have not formed Casparian strips are then induced to do so by externally supplying mono-lignols, leading to formation of Casparian strips within only 6 hours (Naseer et al., 2012) (Figure S3). This allowed us to investigate the immediate effect of NADPH oxidases on Casparian strip formation, uncoupled from their effect on general developmental processes. By co-applying DPI with mono-lignols, we observed a complete block in Casparian strip reconstitution after 6 hours, supporting a direct requirement of NADPH oxidases for lignin polymerisation in the endodermis (Figure 2A). Continued PI uptake confirmed that the endodermal diffusion barrier had not

formed and additionally showed that the DPI concentration and time-scale used did not lead to any cell death, as this would lead to the appearance of strongly PI stained nuclei (Figure 2A, Figure S2).

We then tested whether we could observe production of apoplastic H_20_2 in the endodermis. To do so, we used the Cerium chloride assay. Cerium chloride forms electron-dense precipitates in the presence of H_20_2 through formation of cerium perhydroxide, which can be observed with electron microscopy, providing us with the necessary resolution. With this assay, we observed strikingly localised cerium precipitations in endodermal cells, exclusively at the position of Casparian strips. While early Casparian strips displayed precipitates throughout their width, mature strips only showed signals at their outward-facing edge. The lack of signal at inward facing edges is most probably due to the fact that more mature Casparian strips can function as an apoplastic barrier, not allowing uptake of Cerium choride beyond this point (Figure 2B). 60 min of DPI treatment before Cerium chloride application led to an almost complete absence of local H_20_2, indicating that NADPH oxidases are responsible for this highly localised production of H_20_2 (Figure 2B, Table S3). These findings strongly suggested that an NADPH oxidase is either localised, or locally activated, at the sites of Casparian strip formation.

Regulatory input and localisation determines specificity of RBOHF action

The specific role of RBOHF in Casparian strip formation was surprising, considering that at least one other NADPH oxidase, RBOHB, is strongly expressed in endodermal tissues. (Figure S4). Indeed, insertion lines of RBOHB, or of four other root-expressed NADPH oxidases tested, did not display any delay in Casparian strip formation, nor did double mutants with RBOHF increase the severity of the RBOHF single mutant (Figure 3A). In addition, we recovered six alleles of RBOHF - but no other NADPH oxidase - in our large-scale forward genetic screen (Figure 1A). This strongly suggests that RBOHF plays a unique role in CS formation. A first explanation for its unique function was provided when we localised a complementing fusion construct of RBOHF (mCherry-RBOHF*gen.*) and found that it displayed accumulation in the Casparian strip domain (Figure 3B-D, Figure S5A), while identical fusions of RBOHB and D were excluded from there (Figure 3E). The CSD localisation of RBOHF was surprising, since all other plasma membrane proteins tested so far are excluded from this highly scaffolded domain that even blocks lateral diffusion of lipid tracers like FM4-64 (Alassimone et al., 2010; Roppolo et al., 2011). Therefore, RBOHF entry into this domain probably requires specific interactions between RBOHF and Casparian strip domain proteins like the CASPs. We conclude that differential localisation is one element explaining the apparent specificity of RBOHF. We then generated chimerae between the regulatory and catalytic domains of RBOHB and RBOHF. Intriguingly, the catalytic domain of RBOHB (RBOHB*cat*) can partially rescue the *rbohf* phenotype when it is fused to the RBOHF regulatory domain (RBOHF*reg*). By contrast, a chimera of the RBOHB regulatory domain (RBOHB*reg*), fused to the RBOHF catalytic domain (RBOHF*cat*) was unable to rescue (Figure 3F). Thus, the N-terminal domain of RBOHF is able to receive a regulatory input that allows its activation for Casparian strip formation. This same input cannot be perceived by RBOHB, present in the same cell. When

localising the different chimeric RBOH proteins, we noticed that neither the F*reg*-B*cat* nor the B*reg*-F*cat* chimera accumulated detectably in the Casparian strip Domain, demonstrating that both regulatory and catalytic domain of RBOHF are needed for correct localisation and providing an explanation for the only partial rescue of the RBOHF*reg*-B*cat* chimera (Figure S5C). Therefore, the specific activity of RBOHF is apparently due to a concurrence of correct localisation and ability to receive a specific stimulatory input. Eventually, aberrantly structured Casparian strip will be formed in *rbohf*, suggesting that, in late stages, additional sources of ROS can partially compensate for lack of RBOHF. One possibility is that one of the as yet untested RBOH genes is able to account for this effect.

Peroxidases use localised superoxide-derived H_20_2 for Casparian strip formation

Our model whereby localised RBOHF-mediated superoxide production determines local lignin polymerisation, leads to a number of falsifiable predictions (Figure 4A). First of all, the NADPH oxidase-produced superoxide must be dismutated into H_20_2, often involving catalytic conversion through apoplastic dismutases (Karlsson et al., 2005; Karpinska et al., 2001). Indeed, applying DDC, an inhibitor of dismutases, led to a strong block in Casparian strip recovery in the short-term assay described above for DPI (Figure 4B). Eliminating the local H_20_2 should then lead to a block in Casparian strip formation, and we indeed observed this by treating plants with KI, a scavenger of H_20_2. Finally, only peroxidases require H_20_2, in contrast to the 0_2-requiring Laccases, also known to mediate lignin formation. Therefore, we applied SHAM, which interferes with the haem co-enzyme of peroxidases. Again, we observed a strong block in Casparian strip and diffusion barrier formation (Figure 4C). Neither DDC nor SHAM are very specific inhibitors of their respective enzyme groups and both can have very toxic side-effects. Therefore, care was taken to determine a non-cytotoxic concentration and to assess the effect in the shortest possible time window (Figure S2). It can be seen from the propidium iodide uptake experiments that under our conditions, a block in Casparian strip formation is not simply due to cell death, since propidium iodide quickly penetrates into dead plant cells, leading to a very bright nuclear staining. The fact that three different manipulations - inhibition of dismutases, H_20_2 scavenging, as well as inhibition of peroxidases, all block Casparian strip formation provides additional support to a model in which RBOHF controlled superoxide production supplies H_20_2 for a peroxidase-mediated polymerisation of lignin, forming Casparian strips.

Specific, endodermis-expressed peroxidases are required for Casparian strip formation

In order to obtain additional evidence for this model, we decided to focus on the last step of the process, the peroxidases. Indeed, cell-type specific microarrays show a good number of endodermis-enriched, secreted (type III) peroxidases and co-expression analysis with CASP1 brings up a number of peroxidases at very good scores (Figure 5A). We confirmed endodermis-specific or enriched expression by generating promoter::NLS-GFP fusions of candidate peroxidase genes (Figure 5B, Table S4). Unfortunately, even when we combined four highly endodermis-enriched peroxidases into a quadruple mutant, we could not

observe any delay in the formation of the diffusion barrier (Figure 5C, Table S2). However, one of the peroxidases that is strongly and specifically expressed in the endodermis, PER64, is not represented in available knock-out collections. Therefore, we generated inducible, endodermis-specific artificial microRNA (amiRNA) knock-down lines of this peroxidase (Table S5). To our surprise, we observed a significant delay in diffusion barrier formation when PER64 amiRNA was induced in the wild-type background. This provides some first, genetic evidence for a role of peroxidases in Casparian strip formation and indicates that PER64, probably in conjunction with other, endodermis-expressed peroxidases, is directly required for Casparian strip formation. A localised production of H_20_2 at the Casparian strip domain, as a required co-substrate for peroxidases, could in principle be sufficient for a localised lignin polymerisation, even if the peroxidases themselves were non-localised within the endodermal cell wall space. However, this solution might not be optimal, because H_20_2 diffusion is known to be rapid (Miller et al., 2009) and could thus easily lead to ectopic lignin formation, as would any ectopic, stress-related production of H_20_2, provided lignin precursors are present. We therefore tested whether subcellular localisation of PER64 and other endodermis-expressed peroxidases provides additional spatial specificity.

CASPs determine localisation of an endodermal peroxidase to the Casparian strips

When we localised a mCherry c-terminal fusion of PER64 in a CASP1-GFP background, we observed a stunning, essentially perfect, co-localisation with CASP1-GFP (Figure 6A and B). This co-localisation was not restricted to stages where a mature CSD had been formed (Figure 6B), but could even be observed at very early stages, where CASP1-GFP is still present in a string of isolated micro domains at the plasma membrane (Roppolo et al., 2011) (Figure 6A). This suggests an intimate connection between CASP1 and PER64 subcellular targeting. Other endodermal peroxidases tested also showed an accumulation at the CSD, although none was as specific as PER64 and signals outside of the Casparian strip, such as in cell corners, vacuoles or other intracellular compartments could be observed (Figure S6A). We confirmed that accumulation in the Casparian strip is not a general feature for secreted proteins in the endodermis, by using the extracellular domain of FORMIN HOMOLOGY 1 (FH_{1-107}), which was previously shown to be efficiently secreted and to ubiquitously label the cell wall (Martiniere et al., 2011). At first glance, the FH_{1-107}-mCherry appeared to be localised in a manner similar to the Casparian strips. The non-overlapping distribution with CASP1-GFP, however, clearly showed that FH_{1-107}-mCherry simply accumulates preferentially in the outward facing cell corners of the endodermis, possibly because this part contains by far the most cell wall material (Figure S6B). Whether the difference between PER64 and other peroxidases is due some special property of PER64, such as a better tolerance towards protein fusions remains to be determined. We then decided to ectopically co-express CASP1-GFP and PER64-mCherry in epidermal cells by an inducible promoter in epidermal cells in order to see whether CASP1-GFP is sufficient for localising PER64. Previously, we had shown that CASP misexpression in epidermal cells can lead to strong accumulation of CASPs in structurally aberrant endoplasmic reticulum (ER) (Roppolo et al., 2011).

Intriguingly, when PER64 was co-expressed with CASP1-GFP in the epidermis, both strongly accumulated in the aberrant ER, even though no other endodermis-specific factors are present (Figure 6C, Figure S6C-E). Interestingly, CASP5-GFP, which also induced, and localised to, similar aberrant ER structures was not able to cause intracellular accumulation of PER64, which was secreted in a non-localised fashion to the cell walls of the epidermis (Figure 6D). Moreover, neither epidermal expressed CASP1-GFP, nor CASP5-GFP was able to block secretion of the $FH_{1\text{-}107}$-mCherry control (Figure S6F). In our view, these data are suggestive of an interaction between CASP1 and PER64 and show that CASP1 is sufficient to determine the subcellular localisation of PER64 in epidermal cells. In addition, we could demonstrate that CASPs are also necessary for correct PER64 localisation in the endodermis. In a *casp1 casp3* double-mutant, PER64-mCherry localisation remained in interrupted bands at the location of the Casparian strip domain for a long period, eventually forming contiguous bands, but which appeared broader and more patchy than in the wild-type (Figure 6E) This localisation of the putative lignin-forming PER64 nicely fits with the previously observed, aberrant formation of Casparian strips in this double mutant and additionally supports a role for PER64 in lignin formation (Figure 6F) (Roppolo et al., 2011).

The striking localisation of many endodermis-enriched peroxidases to the Casparian strip strongly suggests that localised peroxidases contribute to the spatially confined formation in the endodermis, together with the localised RBOHF-dependent H_20_2 production. The conjunction of the two localised activities might be necessary to ensure a tight spatial control of the essentially irreversible process of lignin polymerisation.

Discussion

Originally described as being responsible for the so-called respiratory burst in neutrophils, NADPH oxidases in animals are now known to control a vast array of functions. NADPH oxidase-produced ROS has been implicated in various stress signals, but also hormone production, generation of extracellular signaling gradients, or matrix formation (Bedard and Krause, 2007; Moribe et al., 2012; Niethammer et al., 2009). Plants have undergone an independent diversification of NADPH oxidases that mediate a similarly stunning array of functions (Sagi and Fluhr, 2006). Arabidopsis contains 10 Respiratory Burst Homolog (RBOH) genes. Initially described in the context of the oxidative burst during hypersensitive cell death (Torres et al., 2002), RBOHs became rapidly implicated in a more diverse array of signaling pathways and RBOH-dependent ROS has now been established as an important intracellular second messenger that regulates expression of hundreds of genes in response to diverse stimuli, such as cellular damage, drought, salt stress, presence of elicitors, etc. However, the immediate « ROS-receptors » that activate the diverse signaling pathways have remained elusive and it is unclear how specificity of ROS signaling might be controlled (Moller and Sweetlove, 2010; Torres, 2010). While much recent work has focussed on the role of NADPH oxidase-produced ROS in signalling, initial reports described plasma membrane oxidase-produced ROS as an agent involved in cell wall cross-linking (Bradley et al., 1992). Root hair tip growth is one recent example in which a specific NADPH oxidase (RBOHC) was shown to produce ROS for cell wall modification. RBOHC was found to be mutated in the root hair-defective 2 (rhd2) mutant and shown to localise to the growth zone of root hairs. The apoplastic ROS produced by RBOHC is thought to counteract pH-induced cell wall loosening in order to prevent root hair bursting. However, it is unclear which proteins or cell wall polymers are targeted by ROS in this context (Foreman et al., 2003; Monshausen et al., 2007; Takeda et al., 2008).

RBOHF is a versatile signaling module involved in diverse cellular responses

Here, we have provided evidence that RBOHF mediates a very different kind of cell wall modification, not associated with cellular growth. We show that RBOHF is strictly localised within the endodermal plasma membrane, due to its specific N-terminal regulatory domain and its ability to enter the CSD, a highly scaffolded membrane protein platform formed by the CASPs. Localised, extracellular H_20_2 is then used by CASP-recruited peroxidases to mediate mono-lignol oxidation and polymerisation. Absence of RBOHF therefore leads to a very strong delay in the formation of Casparian strips and to an impaired apoplastic barrier. None of the characterised, root expressed RBOHF homologs tested led to a similar phenotype or increased the *rbohf* phenotype in severity, nor did we identify another NADPH oxidase in our forward genetic screen (Alassimone et al., *unpublished*). This specific, non-redundant activity contrasts with the many other, often partially redundant, activities described for RBOHF prior to our work. Initially, RBOHF, together with RBOHD, was shown to be responsible for the ROS burst associated with infection of avirulent bacteria, although RBOHF only made a minor contribution to the detectable ROS burst, while it had a more prominent role in

the induction of cell death (Torres et al., 2002). A very different role for RBOHF in the abscisic acid-induced ROS production in stomata, again in conjunction with RBOHD, was described a year later (Kwak et al., 2003). In this case, the H_20_2 produced is thought to act as a second messenger for activation of calcium channels and MAP kinases (Jammes et al., 2009). Very recently, RBOHF has been found as a salt hypersensitive mutant, necessary for salt-induced ROS production in the stele, which contributes to retention of NaCl from the xylem sap (Jiang et al., 2012). In most reported RBOHF functions, it remains unclear what the direct downstream targets of ROS are and how they relate to the observed phenotypes. Clearly, many reported phenotypes of *rbohf*, such as smaller size, altered cell death response or salt sensitivity could in part be explained as consequences of delayed Casparian strip formation and consequent pleiotropic alterations of nutrient homeostasis. In the future, it will be important to untangle the relationship between the different reported cellular functions and the overall phenotype. This could be done by organ- and cell type-specific complementation assays of RBOHF in stele, root endodermis and stomata, for example. Yet, it remains that RBOHF has multiple different functions in different cells. In stomata, RBOHF receives signals downstream of ABA signaling and RBOHF-produced ROS serves as an intracellular second messenger for the activation of MAP kinases. This is very different role from the localised, apoplastic ROS production for lignin polymerisation that we report here. We speculate that RBOHF, and its homologs, have evolved into versatile signaling modules that can co-exist in the same cell, be specifically activated by diverse inputs and whose outputs – superoxide, dismutated into H_20_2 – will have different activities, depending on their respective subcellular location and the protein components that are assembled around the NADPH oxidase.

CASPs are organisers of cell wall modifying protein activities

We have found that CASP1-GFP co-localises very closely with PER64, as much in the mature Casparian strip domain as during its early assembly. Moreover, ectopically-expressed CASP1 becomes retained in the ER, causing retention of co-expressed PER64 in the same ER structures. This does not occur upon ectopic expression of CASP5, which is equally retained in similar ER bodies, nor are other secreted substrates hindered in their secretion. This specific, induced co-localisation of CASP1 and PER64 is a strong indication of an interaction between CASP1 and PER64. It is most plausible to assume a direct interaction, since indirect interactions would require that « bridging factors » are present in the epidermis and allow interaction of two endodermis-specific proteins. Unfortunately, *in vivo* pull-down experiments are rendered difficult by the polymeric nature of the Casparian strip domain and the tight interaction of both CASPs and peroxidases with the lignified cell wall. Therefore, we have not yet been able to detect interactions between CASPs and peroxidases in such assays (Lee et al., *unpublished*). PER64 is secreted to the apoplast in the epidermis in the absence of CASP1 and shows a broader, patchy distribution in the endodermis of a *casp1 casp3* mutant plant. This shows that PER64 does not require CASP1 for its secretion, but only for its localisation to the Casparian strip domain. Therefore, mutating CASPs should not interfere with lignin polymerisation, but rather lead to a de-localised formation of lignin in the endodermis, which is exactly what is observed in the *casp1 casp3* double-mutant (Roppolo et al., 2011,

this work). We therefore view the function of CASPs – and by extension the large family of CASP-like proteins, as plasma membrane platforms that serve to localise peroxidases – and possibly additional cell wall modifying enzymes - to the right subcellular location. Even in cases where a very restricted formation of lignin is not required, bringing NADPH oxidases into close proximity of peroxidases could provide channeling of the produced ROS towards peroxidases and increase the efficiency of lignin polymerisation. It will be interesting to see whether assembly of « lignin polymerising complexes » by CASPs or CASP-likes will turn out to be a general feature that applies to other lignifying cell types. A scaffolding and channeling of ROS by CASPs could explain how different activities of ROS can be kept separate, a major current problem for our understanding of ROS action (Moller and Sweetlove, 2010; Sagi and Fluhr, 2006).

NADPH oxidase / peroxidase scaffolding - a widespread mechanism ?

The mechanism that we describe of bringing together NADPH oxidases with the downstream ROS-dependent enzymes might also apply to processes in the animal kingdom. It was shown previously in *C. elegans* that DUOX, an animal-specific NADPH oxidase, as well as a peroxidase are involved in collagen cross-linking, necessary for cuticle formation (Edens et al., 2001). Recently, a tetraspanin was shown to be necessary for DUOX activity at the plasma membrane (Moribe et al., 2012). Tetraspanins bear no discernable homology to CASPs, but are also involved in organising membrane microdomains (Charrin et al., 2009). Possibly, tetraspanins could act like CASPs bringing together NADPH oxidase and peroxidase and insure the localised activation of the oxidase. This would be an intriguing case of convergent evolution that could be driven by the strong advantage in restricting ROS availability to a subset of selected ROS-receptors or ROS-dependent enzymes within the cell.

Experimental Procedures

Plant Material and Growth Conditions

Arabidopsis thaliana ecotype Columbia was used for most experiments. For detail of knockout mutants, see Table S1. The *rbohd rbohf* double knockout seeds were obtained from M.A. Torres (Universidad Politécnica de Madrid, Madrid, Spain). Plants were germinated on 1/2 MS (Murashige and Skoog) agar plates after 2 d in dark at 4 °C. Seedlings were grown vertically in Percival chambers at 22 °C, under long days (16-h light/8-h dark), and were used at 5 d after shift to room temperature.

Chemicals

Details of chemicals used in present work are summarized in Table S6.

Transgenic lines

For generation of expression constructs, Gateway Cloning Technology (Invitrogen) was used. For primer details, see Tables S4 and S5. Artificial microRNAs were designed using the Web microRNA Designer (http://wmd2.weigelworld.org) targeting PER64 nucleotides 555-575 of the CDS, and expressed under the estradiol-inducible *CASP1* promoter. Transgenic plants were generated by introduction of the plant expression constructs into an *Agrobacterium tumefaciens* strain GV3101 and transformation was done by floral dipping (Clough and Bent, 1998).

GUS-Staining

For promoter::GUS analysis, 5-d-old seedling were incubated in 5-bromo-4-chloro-3-indolyl-β-D-glucuronide (X-Gluc) staining buffer solution (10 mM EDTA, 0.1% Triton X-100, 2 mM Fe2+CN, 2 mM Fe3+CN, 1 mg/mL X-Gluc) in 50 mM sodium phosphate buffer (pH7.2) at 37 °C for 5~24 h in darkness.

Microscopy and Quantitative Analysis

Confocal laser scanning microscopy was performed on a Zeiss LSM 700 confocal microscope. Excitation and detection windows were set as follows: GFP 488 nm, 500–600 nm; mCherry 594 nm, 600–700 nm; Propidium iodide 488 nm, 600–700 nm; mCitrine and mCherry 514 nm and 594 nm, 520–560 nm and 600–700 nm. Casparian strips were visualized, as described in (Alassimone et al., 2010; Naseer et al., 2012). For visualization of the apoplastic barrier, seedlings were incubated in the dark for 10 min in a fresh solution of 15 µM (10 µg/mL) PI and rinsed two times in water (Alassimone et al., 2010; Naseer et al., 2012). For quantification, “onset of elongation” was defined as the point where an endodermal cell in a median optical section was more than three times its width. From this point, cells in the file were counted until the PI signal was blocked in the endodermal cells.

Inhibitor Treatments

For the treatment of potassium iodide (KI, H_2O_2 Scavenger) and salicylhydroxamic acid (SHAM, peroxidase inhibitor), 5-d-old seedlings were

transferred to the plates containing 5 mM KI or 100 µM SHAM and incubated for 24 h in dark. For the diphenyleneiodonium (DPI, NADPH oxidase inhibitor) and diethyldithiocarbamic acid (DDC, superoxide dismutase inhibitor) treatment, 5-d-old seedlings were pre-incubated in plates containing 10 µM Piperonylic acid (PA, lignin inhibitor) for 24 h in dark and transferred to 1/2 MS solution including 5 µM DPI or 250 µM DDC together with two monolignols: 20 µM of each coniferyl alcohol and sinapyl alcohol.

Transmission Electron Microscopy for cerium chloride (CeCl3)-based H_2O_2 detection

The histochemical method based on the generation of cerium perhydroxides as described in (Bestwick et al., 1997) and was used for the location of H_2O_2 at the Casparian strips. Cerous ions (Ce^{3+}) react with H_2O_2 forming electron dense cerium perhydroxide precipitates which are detected by electron microscopy.

5-d-old seedlings were pre-incubated in 50 mM MOPS [3-(*N*-morpholino) propane sulphonic acid] pH 7.2 alone or with 10 µM DPI for 1 h and then freshly prepared 10 mM $CeCl_3$ was added. After 30 min incubation with $CeCl_3$, plants were washed twice in MOPS for 5 min and then fixed in glutaraldehyde solution (EMS, Hatfield, PA, US) 2.5% in phosphate buffer (PB 0.1M pH7.4) during 1 hour at room temperature (RT). Then, they were post-fixed in a fresh mixture of glutaraldehyde 2.5% in osmium tetroxide 1% (EMS, Hatfield, PA, US) with 1.5% of potassium ferrocyanide (Sigma, St Louis, MO, US) in PB buffer during 1h at RT. The samples were then washed two times in distilled water and dehydrated in acetone solution (Sigma, St Louis, MO, US) at graded concentrations (30%-40min; 50%-40min; 70%-40min; 3x(100%-1h)). This was followed by infiltration in Spurr resin (EMS, Hatfield, PA, US) at graded concentrations (Spurr 33% in acetone-12h; Spurr 66% in acetone-12h, Spurr 2x(100%-8h)) and finally polymerized for 48h at 60°C in oven. Ultrathin sections of 60nm thick were cut transversally at 2mm from the root tip, on a Leica Ultracut (Leica Mikrosysteme GmbH, Vienna, Austria) and picked up on a nickel slot grid 2x1mm (EMS, Hatfield, PA, US) coated with a polystyrene film (Sigma, St Louis, MO, US). Sections were post stained with uranylacetate (Sigma, St Louis, MO, US) 4% in H_2O during 10 minutes, rinsed several times with H_2O followed by Coogeshall lead citrate 0.4% in H_2O (Sigma, St Louis, MO, US) during 10 minutes and rinsed several times with H_2O. Micrographs of the Casparian stripes were taken with a transmission electron microscope FEI CM100 (FEI, Eindhoven, The Netherlands) at an acceleration voltage of 80kV and 24500X of magnification (pixel size of 1.385nm and HFW of 5.55µm) with a Morada SIS digital camera (Olympus Soft Imaging Solutions GmbH, Münster, Germany) using the software SIS iTEM (Olympus Soft Imaging Solutions GmbH, Münster, Germany).

Acknowledgements
We wish to thank M.A. Torres for providing mutant lines and PN Benfey for providing microarray data for analysis. We thank E.M.N. Dohmann, E.E. Farmer, S. Naseer, D.E. Salt and J.E.M. Vermeer for critically reading the manuscript. This work was funded by a European Research Council Young Investigator grant and grants from the Swiss National Science Foundation to N.G. and a European Molecular Biology Organization long-term fellowship to Y.L. Electron microscopy and confocal microscopy were done using expertise and equipment of the Electron Microscopy Facility (EMF) and the Cellular Imaging Facility (CIF) at the University of Lausanne.

References

Alassimone, J., Naseer, S., and Geldner, N. (2010). A developmental framework for endodermal differentiation and polarity. Proc Natl Acad Sci U S A *107*, 5214-5219.

Barcelo, A.R. (1998). The generation of H2O2 in the xylem of Zinnia elegans is mediated by an NADPH-oxidase-like enzyme. Planta *207*, 207-216.

Bedard, K., and Krause, K.H. (2007). The NOX family of ROS-generating NADPH oxidases: physiology and pathophysiology. Physiol Rev *87*, 245-313.

Bergmann, D.C., and Sack, F.D. (2007). Stomatal development. Annu Rev Plant Biol *58*, 163-181.

Berthet, S., Demont-Caulet, N., Pollet, B., Bidzinski, P., Cezard, L., Le Bris, P., Borrega, N., Herve, J., Blondet, E., Balzergue, S*., et al.* (2011). Disruption of LACCASE4 and 17 results in tissue-specific alterations to lignification of Arabidopsis thaliana stems. Plant Cell *23*, 1124-1137.

Bestwick, C.S., Brown, I.R., Bennett, M.H., and Mansfield, J.W. (1997). Localization of hydrogen peroxide accumulation during the hypersensitive reaction of lettuce cells to Pseudomonas syringae pv phaseolicola. Plant Cell *9*, 209-221.

Birnbaum, K., Shasha, D.E., Wang, J.Y., Jung, J.W., Lambert, G.M., Galbraith, D.W., and Benfey, P.N. (2003). A gene expression map of the Arabidopsis root. Science 302, 1956-1960.

Boisson-Dernier, A., Roy, S., Kritsas, K., Grobei, M.A., Jaciubek, M., Schroeder, J.I., and Grossniklaus, U. (2009). Disruption of the pollen-expressed FERONIA homologs ANXUR1 and ANXUR2 triggers pollen tube discharge. Development *136*, 3279-3288.

Bradley, D.J., Kjellbom, P., and Lamb, C.J. (1992). Elicitor- and wound-induced oxidative cross-linking of a proline-rich plant cell wall protein: a novel, rapid defense response. Cell *70*, 21-30.

Brady, S.M., Orlando, D.A., Lee, J.Y., Wang, J.Y., Koch, J., Dinneny, J.R., Mace, D., Ohler, U., and Benfey, P.N. (2007). A high-resolution root spatiotemporal map reveals dominant expression patterns. Science *318*, 801-806.

Charrin, S., Le Naour, F., Silvie, O., Milhiet, P.E., Boucheix, C., and Rubinstein, E. (2009). Lateral organization of membrane proteins: tetraspanins spin their web. Biochemical Journal *420*, 133-154.

Clough, S.J., and Bent, A.F. (1998). Floral dip: a simplified method for Agrobacterium-mediated transformation of Arabidopsis thaliana. Plant J *16*, 735-743.

Cosgrove, D.J. (2005). Growth of the plant cell wall. Nat Rev Mol Cell Biol *6*, 850-861.

Edens, W.A., Sharling, L., Cheng, G., Shapira, R., Kinkade, J.M., Lee, T., Edens, H.A., Tang, X., Sullards, C., Flaherty, D.B.*, et al.* (2001). Tyrosine cross-linking of extracellular matrix is catalyzed by Duox, a multidomain oxidase/peroxidase with homology to the phagocyte oxidase subunit gp91phox. J Cell Biol *154*, 879-891.

Escobar-Restrepo, J.M., Huck, N., Kessler, S., Gagliardini, V., Gheyselinck, J., Yang, W.C., and Grossniklaus, U. (2007). The FERONIA receptor-like kinase mediates male-female interactions during pollen tube reception. Science *317*, 656-660.

Fagerstedt, K.V., Kukkola, E.M., Koistinen, V.V.T., Takahashi, J., and Marjamaa, K. (2010). Cell Wall Lignin is Polymerised by Class III Secretable Plant Peroxidases in Norway Spruce. J Integr Plant Biol *52*, 186-194.

Foreman, J., Demidchik, V., Bothwell, J.H., Mylona, P., Miedema, H., Torres, M.A., Linstead, P., Costa, S., Brownlee, C., Jones, J.D.*, et al.* (2003). Reactive oxygen species produced by NADPH oxidase regulate plant cell growth. Nature *422*, 442-446.

Hematy, K., Cherk, C., and Somerville, S. (2009). Host-pathogen warfare at the plant cell wall. Curr Opin Plant Biol *12*, 406-413.

Jammes, F., Song, C., Shin, D., Munemasa, S., Takeda, K., Gu, D., Cho, D., Lee, S., Giordo, R., Sritubtim, S.*, et al.* (2009). MAP kinases MPK9 and MPK12 are preferentially expressed in guard cells and positively regulate ROS-mediated ABA signaling. Proc Natl Acad Sci U S A *106*, 20520-20525.

Jiang, C., Belfield, E.J., Mithani, A., Visscher, A., Ragoussis, J., Mott, R., Smith, J.A., and Harberd, N.P. (2012). ROS-mediated vascular homeostatic control of root-to-shoot soil Na delivery in Arabidopsis. Embo J *31*, 4359-4370.

Karkonen, A., and Koutaniemi, S. (2010). Lignin Biosynthesis Studies in Plant Tissue Cultures. J Integr Plant Biol *52*, 176-185.

Karlsson, M., Melzer, M., Prokhorenko, I., Johansson, T., and Wingsle, G. (2005). Hydrogen peroxide and expression of hipI-superoxide dismutase are associated

with the development of secondary cell walls in Zinnia elegans. Journal of Experimental Botany *56*, 2085-2093.

Karpinska, B., Karlsson, M., Schinkel, H., Streller, S., Suss, K.H., Melzer, M., and Wingsle, G. (2001). A novel superoxide dismutase with a high isoelectric point in higher plants. Expression, regulation, and protein localization. Plant Physiology *126*, 1668-1677.

Kim, S.H., Turnbull, J., and Guimond, S. (2011). Extracellular matrix and cell signalling: the dynamic cooperation of integrin, proteoglycan and growth factor receptor. J Endocrinol *209*, 139-151.

Kwak, J.M., Mori, I.C., Pei, Z.M., Leonhardt, N., Torres, M.A., Dangl, J.L., Bloom, R.E., Bodde, S., Jones, J.D., and Schroeder, J.I. (2003). NADPH oxidase AtrbohD and AtrbohF genes function in ROS-dependent ABA signaling in Arabidopsis. Embo J *22*, 2623-2633.

Liu, C.J. (2012). Deciphering the enigma of lignification: precursor transport, oxidation, and the topochemistry of lignin assembly. Mol Plant *5*, 304-317.

Martiniere, A., Gayral, P., Hawes, C., and Runions, J. (2011). Building bridges: formin1 of Arabidopsis forms a connection between the cell wall and the actin cytoskeleton. Plant J *66*, 354-365.

Miller, G., Schlauch, K., Tam, R., Cortes, D., Torres, M.A., Shulaev, V., Dangl, J.L., and Mittler, R. (2009). The plant NADPH oxidase RBOHD mediates rapid systemic signaling in response to diverse stimuli. Sci Signal *2*, ra45.

Miyazaki, S., Murata, T., Sakurai-Ozato, N., Kubo, M., Demura, T., Fukuda, H., and Hasebe, M. (2009). ANXUR1 and 2, sister genes to FERONIA/SIRENE, are male factors for coordinated fertilization. Curr Biol *19*, 1327-1331.

Moller, I.M., and Sweetlove, L.J. (2010). ROS signalling--specificity is required. Trends Plant Sci *15*, 370-374.

Monshausen, G.B., Bibikova, T.N., Messerli, M.A., Shi, C., and Gilroy, S. (2007). Oscillations in extracellular pH and reactive oxygen species modulate tip growth of Arabidopsis root hairs. Proc Natl Acad Sci U S A *104*, 20996-21001.

Moribe, H., Konakawa, R., Koga, D., Ushiki, T., Nakamura, K., and Mekada, E. (2012). Tetraspanin Is Required for Generation of Reactive Oxygen Species by the Dual Oxidase System in Caenorhabditis elegans. PLoS Genet *8*, e1002957.

Naseer, S., Lee, Y., Lapierre, C., Franke, R., Nawrath, C., and Geldner, N. (2012). Casparian strip diffusion barrier in Arabidopsis is made of a lignin polymer without suberin. Proc Natl Acad Sci U S A *109*, 10101-10106.

Niethammer, P., Grabher, C., Look, A.T., and Mitchison, T.J. (2009). A tissue-scale gradient of hydrogen peroxide mediates rapid wound detection in zebrafish. Nature *459*, 996-999.

Oda, Y., and Fukuda, H. (2012a). Initiation of cell wall pattern by a Rho- and microtubule-driven symmetry breaking. Science *337*, 1333-1336.

Oda, Y., and Fukuda, H. (2012b). Secondary cell wall patterning during xylem differentiation. Curr Opin Plant Biol *15*, 38-44.

Pesquet, E., Korolev, A.V., Calder, G., and Lloyd, C.W. (2010). The Microtubule-Associated Protein AtMAP70-5 Regulates Secondary Wall Patterning in Arabidopsis Wood Cells. Curr Biol.

Roppolo, D., De Rybel, B., Tendon, V.D., Pfister, A., Alassimone, J., Vermeer, J.E., Yamazaki, M., Stierhof, Y.D., Beeckman, T., and Geldner, N. (2011). A novel protein family mediates Casparian strip formation in the endodermis. Nature *473*, 380-383.

Sagi, M., and Fluhr, R. (2006). Production of reactive oxygen species by plant NADPH oxidases. Plant Physiol *141*, 336-340.

Swanson, S., and Gilroy, S. (2010). ROS in plant development. Physiol Plant *138*, 384-392.

Takeda, S., Gapper, C., Kaya, H., Bell, E., Kuchitsu, K., and Dolan, L. (2008). Local positive feedback regulation determines cell shape in root hair cells. Science *319*, 1241-1244.

Torres, M.A. (2010). ROS in biotic interactions. Physiol Plant *138*, 414-429.

Torres, M.A., Dangl, J.L., and Jones, J.D. (2002). Arabidopsis gp91phox homologues AtrbohD and AtrbohF are required for accumulation of reactive oxygen intermediates in the plant defense response. Proc Natl Acad Sci U S A *99*, 517-522.

Vanholme, R., Van Acker, R., and Boerjan, W. (2010). Potential of Arabidopsis systems biology to advance the biofuel field. Trends Biotechnol *28*, 543-547.

Figure Legends

Figure 1. Casparian Strip formation is delayed in *sgn4/rbohf* mutants.
(A) A diagram of RBOHF genomic region shows insertion site of the T-DNA and the positions of the different stop- and missense mutations identified in the six *sgn4* alleles (see also Table S1 and S2).
(B) Apoplastic diffusion barrier was visualized by block of penetration of externally applied propidium iodide (PI, 15 μM) into the stele. Quantification was done by counting endodermal cells after "onset of elongation", defined when an endodermal cell in a median optical section was at least three times its width. From this point, cells in the file were counted until the PI signal was blocked at endodermal cells (5-day old seedlings, mean ± SD, $21 < n < 31$).
(C) Casparian strip networks are visualized as auto fluorescence after clearing in different developmental stages which are represented by counts of endodermal cells after "onset of elongation" (see above). Pictures are maximum projections of longitudinal, surface-to-median confocal image stacks, allowing visualization of the net-like nature of the Casparian strips. Note that xylem vessels are also observed as brightly fluorescent spiral structures.
(D) pCASP1::CASP1-GFP localizes at the net-like Casparian Strip membrane Domain (CSD) in wild-type and *rbohf*. Projections as in C (see also Figure S1). Scale bars: 10 μm.

Figure 2. NADPH oxidase is essential for Casparian strip formation and localized ROS production.
(A) The NADPH oxidase inhibitor, diphenyleneiodonium (DPI) abolishes complementation observed by monolignol addition in the newly grown root zone of 6-day old seedlings. Roots were treated for 24 h with lignin biosynthesis inhibitor piperonylic acid (PA). After this, seedling roots were incubated for 6 hours on plates with monolignols (20 μM coniferyl and sinapyl alcohol) with or without 5 μM DPI. Casparian strip networks (*cell wall autofluorescence, upper panel)* and diffusion barrier formation (*PI tracer uptake, lower panel*) were assessed (see also Figure S2 and S3). **en**: endodermis, **stele**: cell layers enclosed by endodermis
(B) Localized H_2O_2 is detected in electron micrographs by its reaction with 10 mM cerium chloride (CeCl3) to produce electron-dense deposits. 10 μM DPI was pre-treated for 1 hour. Arrows point to electron-dense deposits. Note the deposits are formed throughout CS region in developing strips, but are confined to outer edge of more established strips, probably reflecting block of cerium chloride uptake by the strip itself (see also Table S3). Scale bars (A), 10 μm; (B), 0.5 μm.

Figure 3. **CSD localization and regulatory input determine specificity of RBOHF action in Casparian strip formation.**
(A) Establishment of a functional diffusion barrier is visualized by block of PI diffusion (mean ± SD, $13<n<31$) (see also Figure S4 and Table S2).
(B) Line of mCherry-RBOHF genomic construct, driven by own promoter shows localisation at the plasma membrane and expresses in every cell type of 5-day

old seedling roots, including endodermis where it accumulates at the CSD. Arrowhead points to CSD accumulation (see also Figure S5).
(C) Delayed PI block phenotype of *rbohf* is complemented in three independent complementation lines expressing pRBOHF::mCherry-RBOHF genomic construct (comple-1-3) (mean ± SD, 20<n<31).
(D) Rescued Casparian strip autofluorescence in a complementation line.
(E) Endodermal localization of mCitrine fused to RBOHB, D and F under the CASP1 promoter. Only mCitrine-RBOHF localizes at the Casparian strip membrane domain (CSD). Arrowheads point to CSD (see also Table S5).
(F) Delayed PI-block phenotype of *rbohf* is complemented by introduction of Cit-RBOHF CDS under the CASP1 promoter. When N-terminal regulatory domain of RBOHF is replaced by that of RbohB (Cit-RBOHB***reg***-F***cat***), no complementation is observed. By contrast, regulatory domain of RBOHF combined with catalytic domain of RbohB (Cit-RBOHF***reg***-B***cat***) shows partial complementation ($p < 0.01$, mean ± SD, 19<n<31) (see also Figure S5C). Scale bars (B and D), 10 μm; (E) 5 μm. ep: epidermis, ct: cortex, en: endodermis, st: stele

Figure 4. NADPH oxidase drives H_2O_2 production for peroxidase-mediated lignin polymerization in Casparian strips.
(A) Schematic representation of the required steps between NADPH oxidase activity and lignin polymerization. Diphenyleneiodonium (DPI, NADPH oxidase inhibitor), Diethyldithiocarbamic acid (DDC, Superoxide dismutase inhibitor), Potassium iodide (KI, H_2O_2 scavenger), salicylhydroxamic acid (SHAM, peroxidase inhibitor).
(B) When 250 μM DDC is applied together with monolignols after 24 h of PA treatment, as in Figure 2A, Casparian strip reconstitution does not occur (See also Figure S2 and Table S6).
(C) When 5 mM KI and 100 μM SHAM is applied for 24 h, root growth continues, but Casparian strip formation is inhibited in the newly grown root zone (See also Figure S2 and Table S6). Scale bars (B and C), 10 μm.

Figure 5. Peroxidases are involved in the Casparian strip formation.
(A) Microarray data showing endodermis-enriched gene expression of CASP1 and peroxidases in roots (data from Birnbaum et al., 2003; Brady et al., 2007).
(B) Promoter gene expression analysis of peroxidases with nuclear-localized GFP-GUS as reporter confirms endodermis-specific/enriched gene expression in the endodermis. Arrowheads point to cell layers showing expression. en: endodermis, st: stele (see also Table S4).
(C) Establishment of a functional diffusion barrier, visualized by PI, is not affected in the quadruple mutant of *per3 per9 per39 per72* ($p > 0.5$, mean ± SD, 25<n<29) (see also Table S2).
(D) Establishment of a functional diffusion barrier is delayed in mutants expressing inducible artificial microRNA for PER64 germinated in 1/2 MS plates including 10 μM Estradiol ($p < 0.001$, mean ± SD, 16<n<27) (see also Table S5). Scale bar: 20 μm.

Figure 6. CASP1-GFP determines PER64-mCherry localization.

(A, B) PER64-mCherry driven by own promoter co-localizes with CASP1-GFP in early endodermal cells (A) and later stage of endodermal cells (B) (See also Figure S6A-B and TableS5).
(C, D) Ectopically expressed PER64-mCherry, CASP1-mCitrine, and CASP5-GFP. PER64-mCherry co-localizes at the CASP1-mCitrine aberrant ER structures (C), but not at the CASP5-GFP aberrant ER structures (D) (See also Figure S6C-F).
(E) pPER64::PER64-mCherry in *casp1-1;casp3-1* mutant shows irregular localization of PER64 which is correlated with the pattern of CS autofluorescence in double mutant.
(F) Casparian strip formation defects of *casp1-1;casp3-1* mutant follows the defects of PER64-mCherry localization, with irregular, non-contiguous patches early (~16. cell) and more diffuse autofluorescence later (~22. cell). Scale bars: 10 μm.

Fig. 1

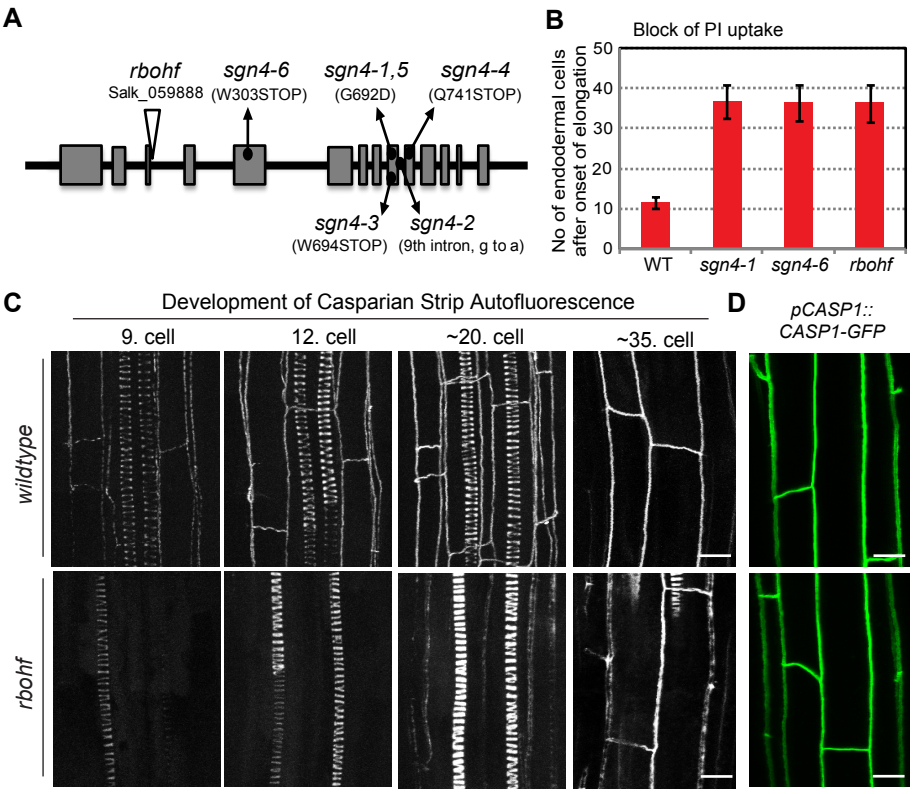
A
rbohf
Salk_059888
sgn4-6
(W303STOP)
sgn4-1,5
(G692D)
sgn4-4
(Q741STOP)
sgn4-3
(W694STOP)
sgn4-2
(9th intron, g to a)
B
Block of PI uptake
No of endodermal cells after onset of elongation
0
10
20
30
40
50
WT
sgn4-1
sgn4-6
rbohf
C
Development of Casparian Strip Autofluorescence
9. cell
12. cell
~20. cell
~35. cell
wildtype
rbohf
D
pCASP1::
CASP1-GFP

Fig. 2

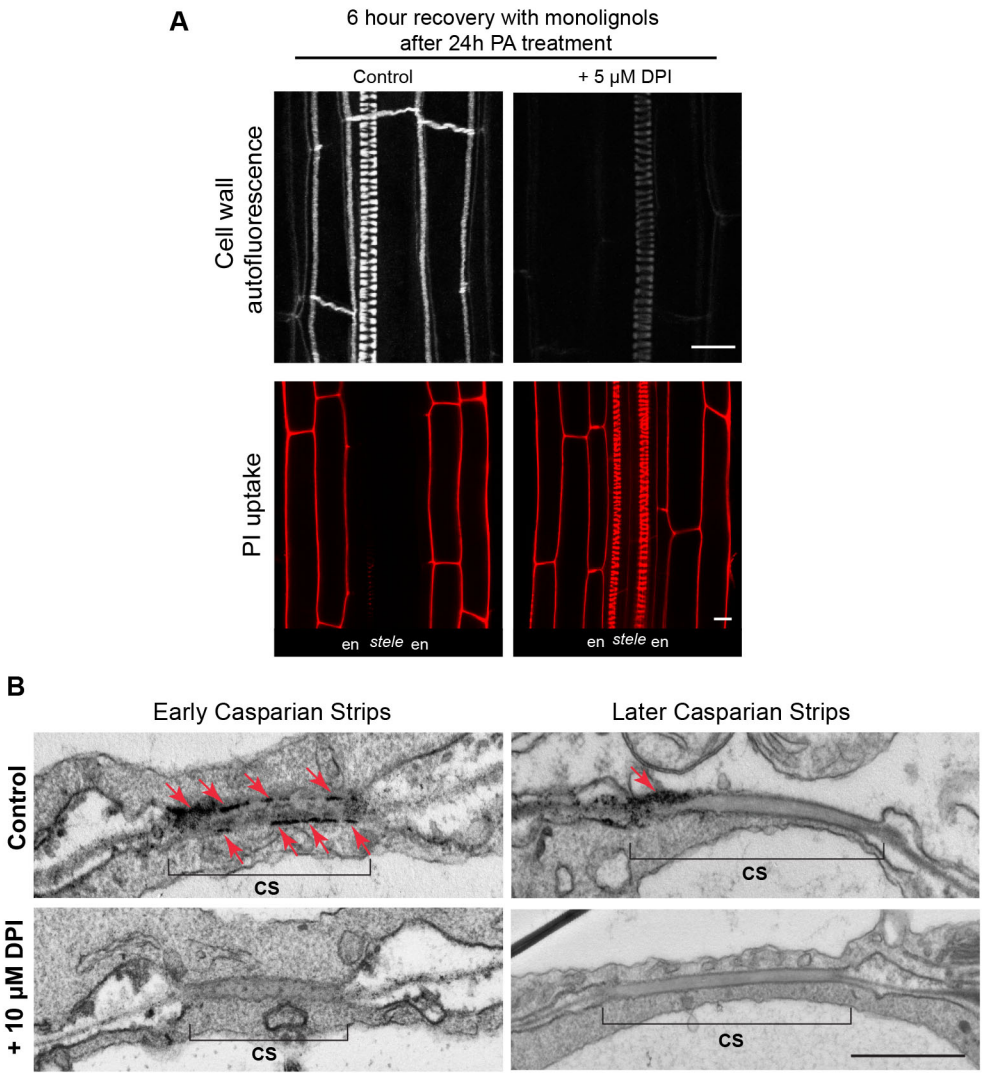
A
6 hour recovery with monolignols
after 24h PA treatment
Control
+ 5 µM DPI
Cell wall
autofluorescence
PI uptake
en stele en
en stele en
B
Early Casparian Strips
Later Casparian Strips
Control
+ 10 µM DPI
CS
CS
CS
CS

Fig. 3

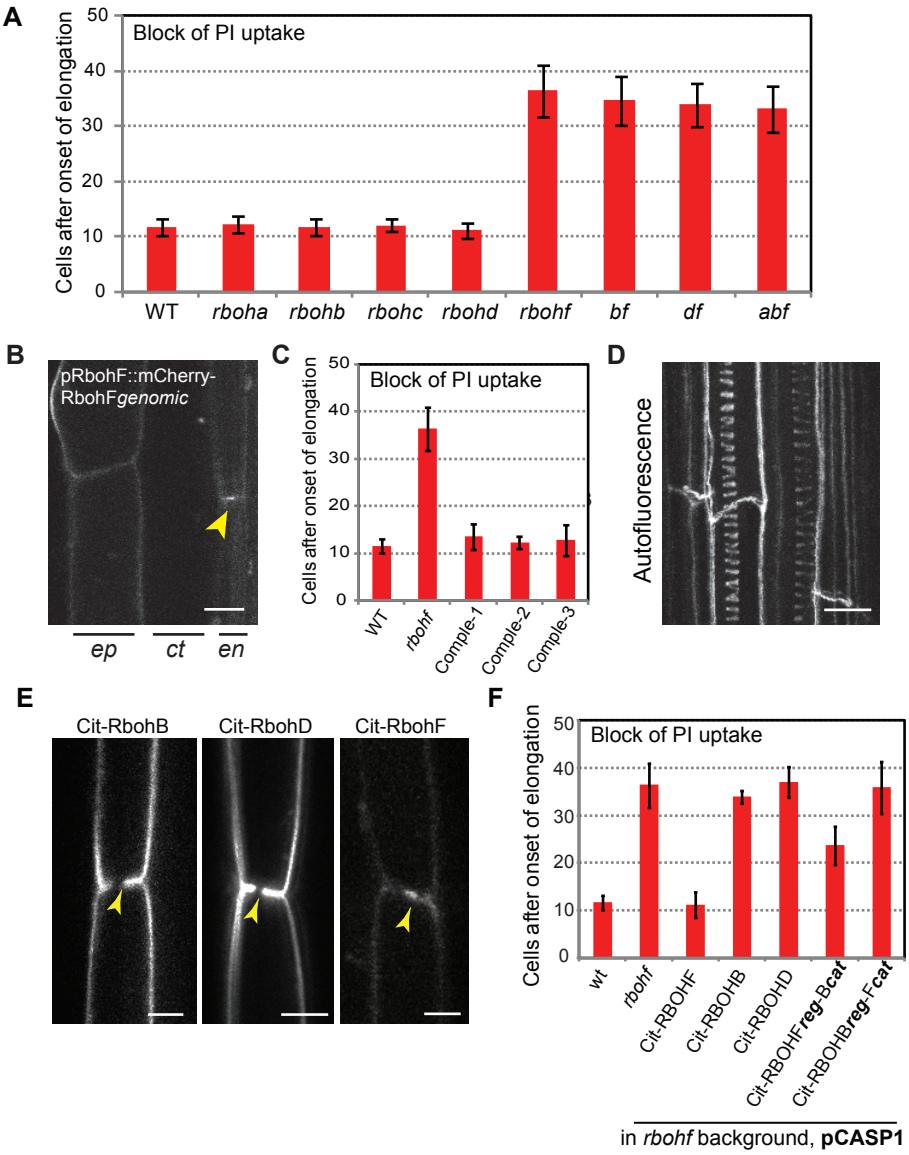
A
Block of PI uptake
Cells after onset of elongation
50
40
30
20
10
0
WT
rboha
rbohb
rbohc
rbohd
rbohf
bf
df
abf
B
pRbohF::mCherry-RbohFgenomic
ep
ct
en
C
Block of PI uptake
Cells after onset of elongation
WT
rbohf
Comple-1
Comple-2
Comple-3
D
Autofluorescence
E
Cit-RbohB
Cit-RbohD
Cit-RbohF
F
Block of PI uptake
Cells after onset of elongation
wt
rbohf
Cit-RBOHF
Cit-RBOHB
Cit-RBOHD
Cit-RBOHFreg-Bcat
Cit-RBOHBreg-Fcat
in rbohf background, pCASP1

Fig. 4

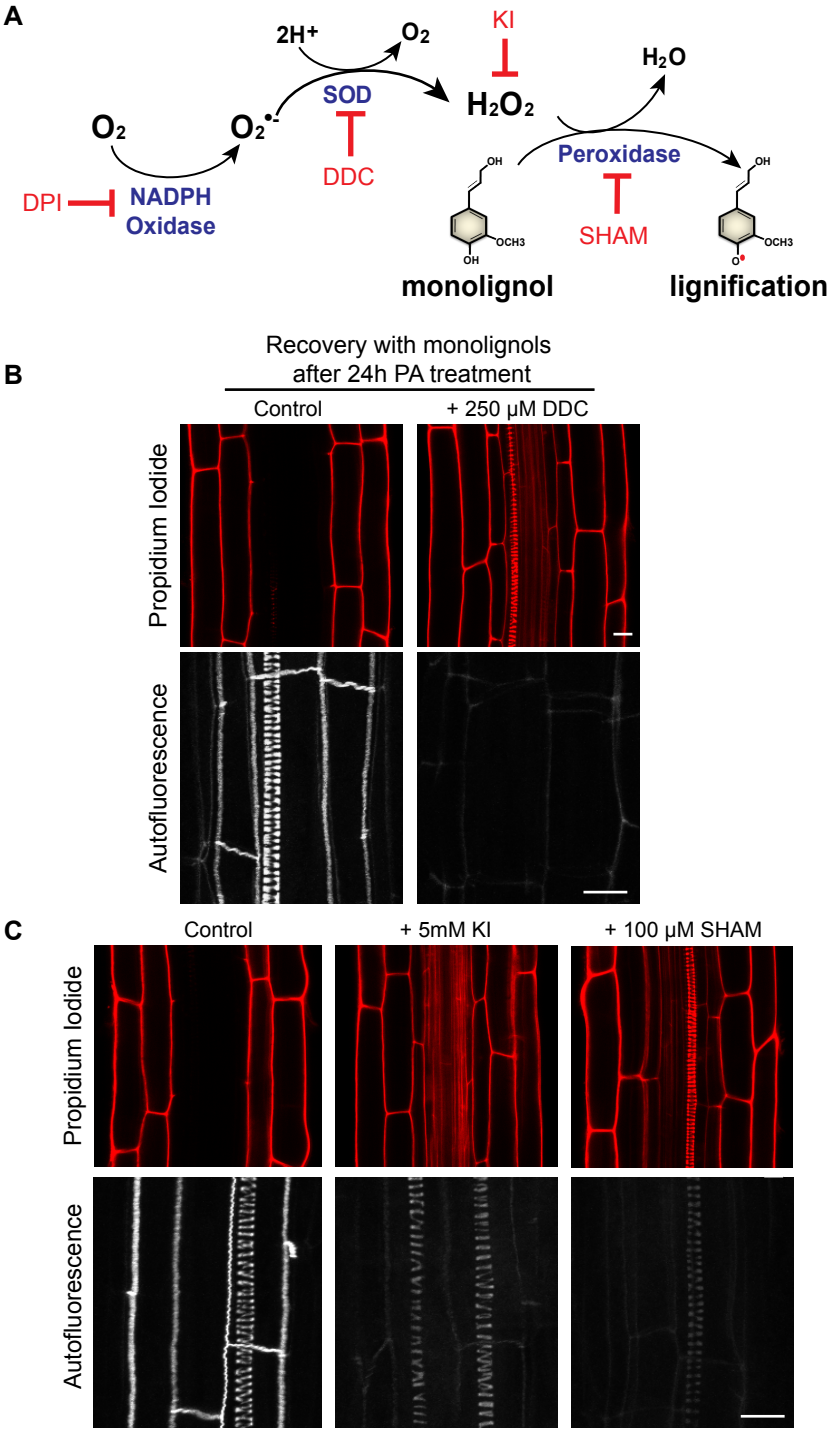
A
2H+
O2
KI
SOD
H2O2
H2O
O2
O2•-
DDC
Peroxidase
DPI
NADPH Oxidase
SHAM
monolignol
lignification
B
Recovery with monolignols after 24h PA treatment
Control
+ 250 µM DDC
Propidium Iodide
Autofluorescence
C
Control
+ 5mM KI
+ 100 µM SHAM
Propidium Iodide
Autofluorescence

Fig. 5

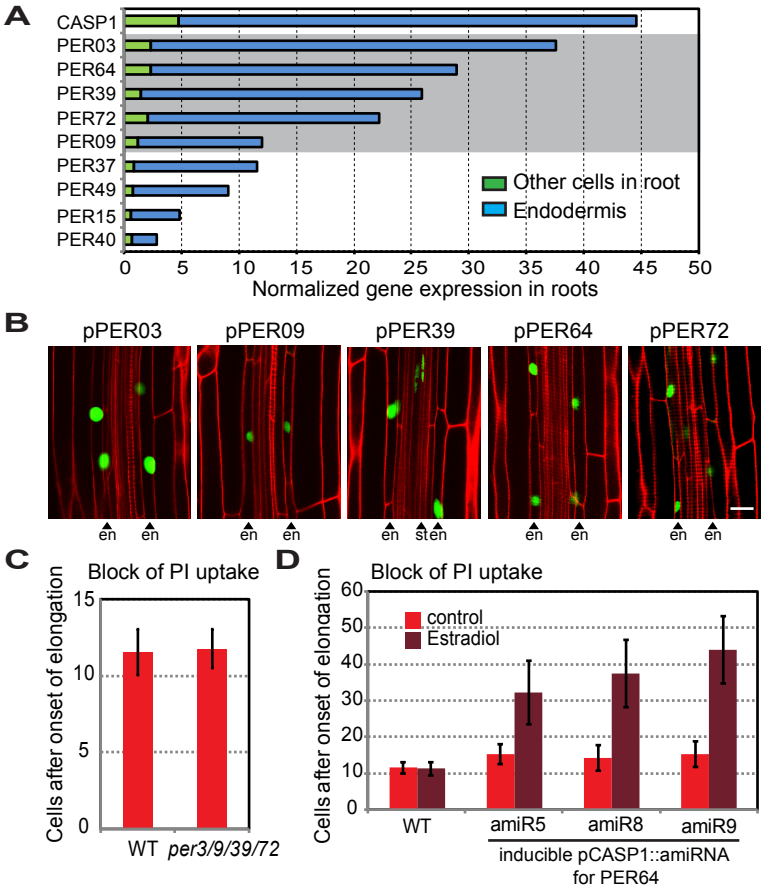
A
CASP1
PER03
PER64
PER39
PER72
PER09
PER37
PER49
PER15
PER40
Other cells in root
Endodermis
0 5 10 15 20 25 30 35 40 45 50
Normalized gene expression in roots
B
pPER03
pPER09
pPER39
pPER64
pPER72
en
en
en
en
en
sten
en
en
en
en
C
Block of PI uptake
Cells after onset of elongation
15
10
5
0
WT per3/9/39/72
D
Block of PI uptake
Cells after onset of elongation
60
50
40
30
20
10
0
control
Estradiol
WT
amiR5
amiR8
amiR9
inducible pCASP1::amiRNA
for PER64

Fig. 6

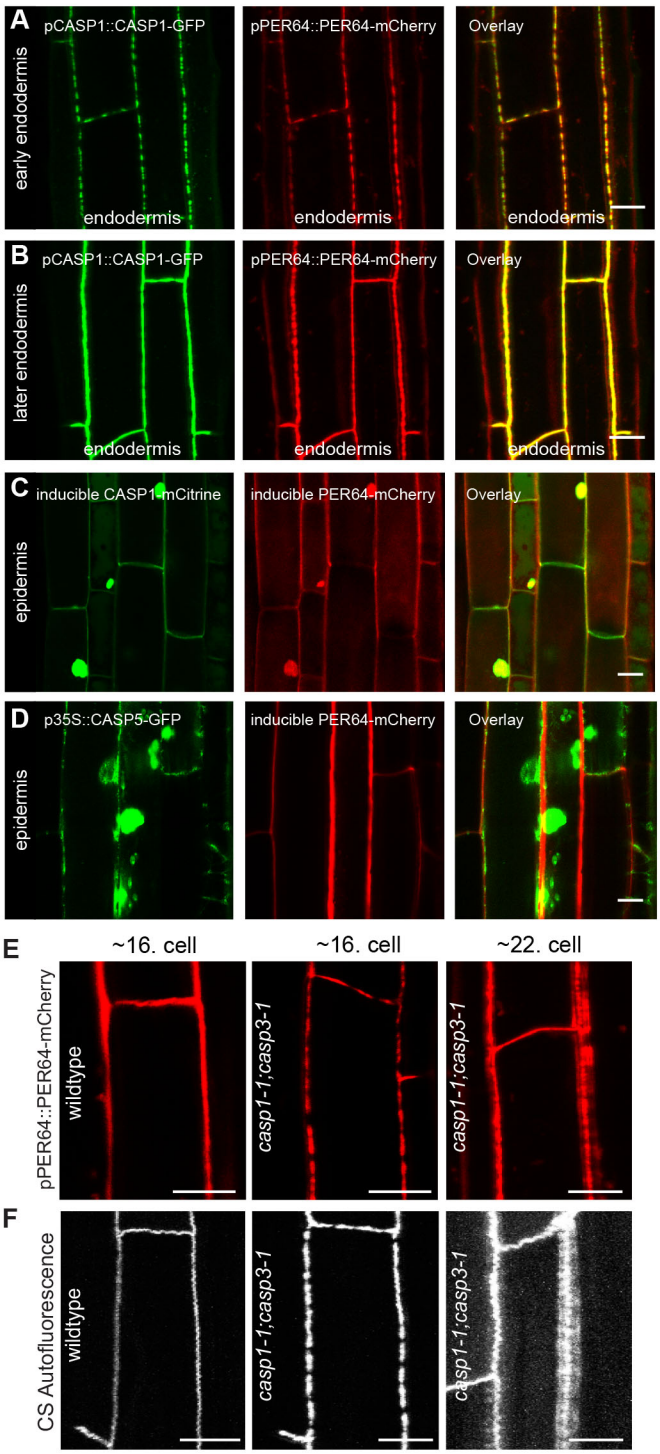
A
pCASP1::CASP1-GFP
pPER64::PER64-mCherry
Overlay
early endodermis
endodermis
endodermis
endodermis
B
pCASP1::CASP1-GFP
pPER64::PER64-mCherry
Overlay
later endodermis
endodermis
endodermis
endodermis
C
inducible CASP1-mCitrine
inducible PER64-mCherry
Overlay
epidermis
D
p35S::CASP5-GFP
inducible PER64-mCherry
Overlay
epidermis
E
~16. cell
~16. cell
~22. cell
pPER64::PER64-mCherry
wildtype
casp1-1;casp3-1
casp1-1;casp3-1
F
CS Autofluorescence
wildtype
casp1-1;casp3-1
casp1-1;casp3-1